The Malaysian Journal of Analytical Sciences, Vol 12, No 3 (2008): 600 - 608

POTENTIOSTATIC DEPOSITION OF COPPER INDIUM DISULFIDE THIN FILMS: EFFECT OF CATHODIC POTENTIALS ON THE OPTICAL AND PHOTOELECTROCHEMICAL PROPERTIES

Teo Sook Liang, Zulkarnain Zainal*, Tan Wee Tee and Imad Hamadneh

Department of Chemistry, Faculty of Science, Universiti Putra Malaysia,
43400 Serdang, Selangor, Malaysia.

** Corresponding author: zulkar@fsas.upm.edu.my*

Abstract

$CuInS_2$ thin films were one-step potentiostatically deposited onto indium tin oxide (ITO) coated glass from aqueous solution containing $CuCl_2$, $InCl_3$ and $Na_2S_2O_3$. The effect of cathodic potentials on the structural, photoelectrochemical and optical properties of the deposited film were studied. X-ray diffraction (XRD) patterns showed that the deposited $CuInS_2$ material was polycrystalline with tetragonal structure. Photoactivity of the samples was studied using linear sweep voltammetry. A typical increase from 1.25 to 2.30 eV in the optical band gap energy was observed on increasing the cathodic potential from -0.30 to -0.70 V (Ag/AgCl).

Keywords: $CuInS_2$; Potentiostatic deposition; Cathodic potential; Photoactivity; Band gap

Introduction

Development and fabrication of solar cells and solid state electronics are basically based on the thin films technology. Thin films are considered as one of the required semiconductor material to build up a photovoltaic cell and some electronic devices. Thin film photovoltaic devices have high worldwide demand to generate an efficient, renewable and clean solar energy as fossil fuel sources will be exhausted in future [1]. Nowadays, more attentions are focusing on the ternary metal chalcogenides semiconductors which are more interesting and have industry potential. Among the ternary I-III-VI_2 semiconductor, $CuInS_2$ has recently drawn considerable a promising material as absorber layer in photovoltaic devices because it has direct band gap of about 1.5 eV which is lies in the optimum spectrum range for solar energy conversion (10.8-11.4%), high absorption coefficient (10^5 cm^{-1}) and good stability for solar radiation. Beside, adjustment of $CuInS_2$ stoichiometric deviation can results both in n- and p-type which is an advantage for either homojunction or heterojunction solar cells [2]. Previous study also showed that indium-rich films may lead to the formation of n-type $CuInS_2$, while copper-rich may result in p-type $CuInS_2$ [3]. In addition, $CuInS_2$ can be synthesized in an environment friendly atmosphere because it does not contain any toxic elements like Se, Te, etc [4]. Thus, threaten to the environment in term of chemical toxicity can be minimized.

Many deposition methods have been developed for the preparation of $CuInS_2$ thin films, such as sulfurization of eletrodeposited Cu-In precursor, wet chemical route, chemical bath deposition, chemical vapour deposition, spray pyrolysis, ion plating, ion layer gas reaction (ILGAR) and co-evaporation [5].Among the various deposition techniques, electrodeposition is the most suitable for the commercial and large scale application. Electrodeposition is an attractive technique and has widely been employed for the deposition of elemental, binary, intermetallic, ternary or even more complex compound and alloy thin films. It is an isothermal process mainly controlled by electrical parameters which are easily adjusted to control thickness, microstructure and composition [6].

Experimental

Deposition of films

Cyclic voltammetry experiment and potentiostatic deposition were carried out using a μ-type III AUTOLAB potentiostat driven by General Purpose Electrochemical System (GPES) software. A three electrode-cell was used, where Ag/AgCl as the reference electrode, ITO-coated glass (4 cm^2) as the working electrode (cathode) and platinum wire as the counter electrode (anode). The substrates and the counter electrode were cleaned with acetone, sodium hydroxide and followed by deionized water using ultrasonic bath. The deposition bath consisted of 20 cm^3 0.01 M $CuCl_2$ (Fisher), 20 cm^3 0.01 M $InCl_3$ (Fluka) and 20 cm^3 0.02 M $Na_2S_2O_3$ (Ajax) and the pH was maintained at 1.50 using 1.00 M HCl. The roles of the HCl are to generate elemental sulfur and reduce the chances of formation of hydroxyl and insoluble compounds. The deposition bath was deaerated using nitrogen gas for ten minutes to create N_2 atmosphere layer on the top of the solution bath. The mixing of solutions must be carried out just before the deposition started to avoid aging of the colloid and the precipitation of sulfur in the cell. While the experiment in progress, a layer of N_2 gas must be provided on top of the surface of the electrolyte solution to prevent oxygen from entering the solution. Cyclic voltammetry experiment was run between two potentials limits (-1.00 V to +1.00 V) with scan rate of 20 mV/s on the cell containing individual 0.01 M $CuCl_2$, 0.01 M $InCl_3$, 0.01 M $Na_2S_2O_3$ and mixture of them. Then, the films were deposited through chronoamperometry technique at potential -0.30 V to -0.70 V for 1800 s.

Films Characterizations

All the deposited films were rinsed with deionized water and kept for further characterization. The films were analyzed using a Philips PM 1730 with Cu Kα radiation of wavelength 1.54 Å for 2θ range from 20^o to 60^o. Photoelectrochemical experiments were performed by running linear sweep voltammetry (LSV) between two potential limits (0 to -1.00 V). The electrodes were immersed in electrolyte bath comprising of 0.01 M $Na_2S_2O_3$. A tungsten halogen lamp (300 W, 120 V) was used for illuminating the electrode and the intensity was controlled by a variable transformer. The light was manually chopped at a constant frequency to give the effect of dark and illumination. The optical behavior study was carried out using Perkin-Elmer Lamda 20 UV-visible spectrometer with blank ITO-coated glass as a reference. The raw data of absorption was manipulated using Stern equation to determine band gap energy and transition type.

Results and Discussion

Cyclic voltammetry experiment

Cyclic voltammetry (CV) was used to study the electrochemical redox reactions of the electrolytes. CV was also performed to study the effect of the applied potentials and subsequently probe the most suitable potential for the deposition. Forward scan was run from +1.00 V to -1.00 V. From Figure 1, in $CuCl_2$ solution, higher over potential at 1.50 V was required at reverse scan for the formation of thermodynamically stable nuclei on ITO-coated glass substrate. The oxidation of copper metal started at around -0.20 V and a peak was observed at 1.00 V versus Ag/AgCl. $Na_2S_2O_3$ is a nonelectroactive species where the current is small for all potentials sweep range. No deposition was observed on the substrate. For the $InCl_3$, a clear anodic peak was formed at -0.40 V which was due to oxidation of In to In^{3+}. Voltammetric curve of the mixture shows cathodic peak begins at -0.80 V due to nucleation loops and hydrogen evolution. Hydrogen evolution is suppressed by thiosulfate decomposition [7]. This was signified by pungent odor imparted from the electrolyte bath. Stronger hydrogen evolution occurred at more negative potential. The formation of hydrogen evolution can be explained as follows:

$$S_2O_3^{2-} + 6H^+ + 4e \rightarrow 2S + 3H_2O \qquad (1)$$

$$2H^+ + 2e \rightarrow H_2 \qquad (2)$$

$$S + 2H^+ + 2e \rightarrow H_2S \qquad (3)$$

Two anodic stripping peaks were resulted at 0.30 V and 0.70 V according to the following reactions:

$$Cu \rightarrow Cu^+ + e \qquad \text{first peak} \qquad (4)$$

$$Cu^+ \rightarrow Cu^{2+} + e \qquad \text{second peak} \qquad (5)$$

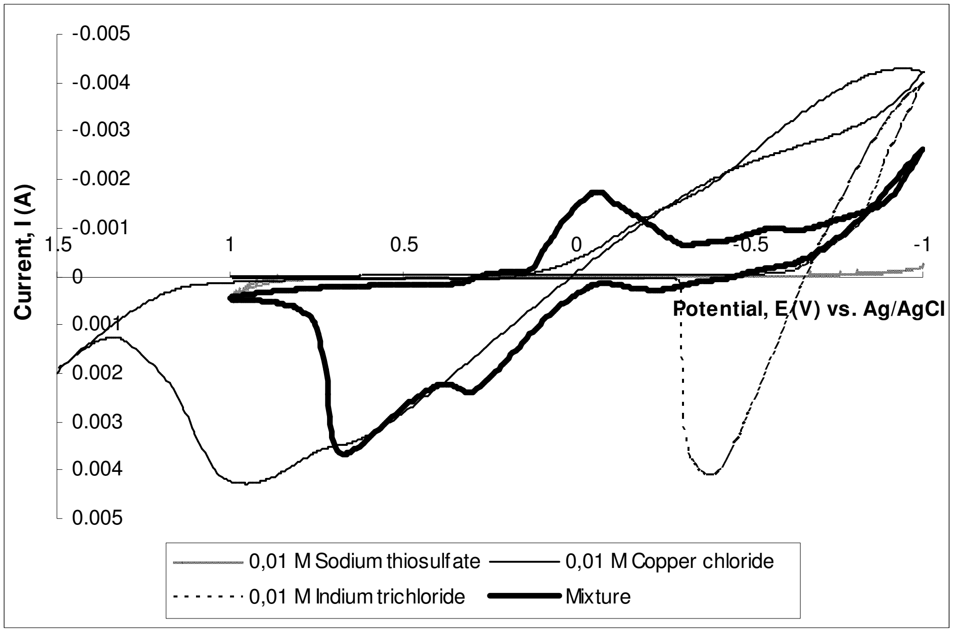

Fig. 1: Voltammetry curves obtained in $CuCl_2$, $InCl_3$, $Na_2S_2O_3$ solutions and their mixture.

Nucleation and growth mechanism

The potentiostatically deposited $CuInS_2$ thin films on ITO-coated glass is most likely caused by the following reactions:

$$Cu^{2+} + 2e \rightarrow Cu \qquad E^o(SHE) = 0.337\ V \qquad (6)$$

$$In^{3+} + 3e \rightarrow In \qquad E^o(SHE) = -0.342\ V \qquad (7)$$

$$HSO_3^- + 5H^+ + 4e \rightarrow S + 3H_2O \qquad E^o(SHE) = 0.420\ V \qquad (8)$$

Thiosulfate ions play a double role in this system: it is a complexing agent for the copper ions, and it is a sulfur source [8]. $Na_2S_2O_3$ is a reducing agent by virtue of half cell reaction:

$$2S_2O_3^{2-} \rightarrow S_4O_6^{2-} + 2e \qquad (9)$$

The solution gradually becomes turbid due to the decomposition of $S_2O_3^{2-}$ ions forming colloidal sulfur. This was corresponding to following chemical reaction:

$$S_2O_3^{2-} + H^+ \rightarrow S + HSO_3^- \qquad (10)$$

Potentiostatic deposition of $CuInS_2$ basically involves three steps: (a) the diffusion of ions from bulk electrolytic solution to the electrode surface and their adsorption at the growth sites at the electrode surface. (b) the reduction of adsorbed ions at the cathode. (c) the migration of reduced copper, indium and sulfur atoms to reactive sites and their solid state reaction [9].

$$x\text{Cu} + y\text{In} + z\text{S} \rightarrow \text{Cu}_x\text{In}_y\text{S}_z \qquad (11)$$

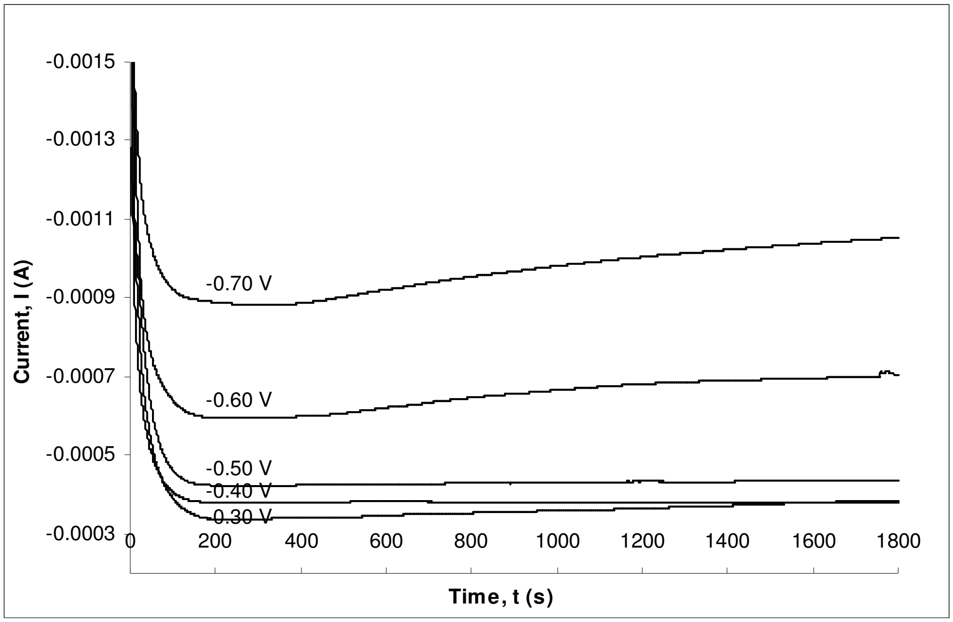

Fig. 2: I-t curves measured at different cathodic deposition potentials.

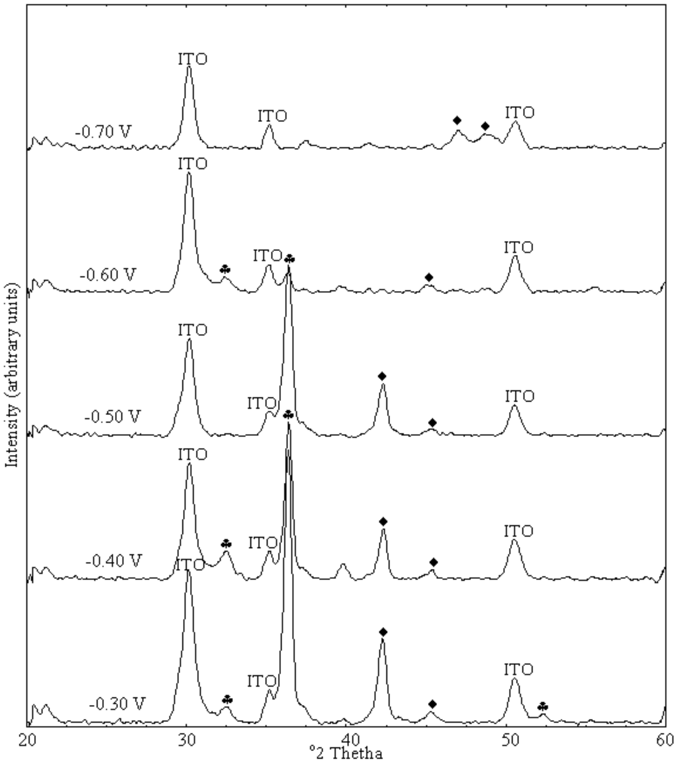

Fig. 3: XRD pattern of the samples prepared at different deposition potentials.
$CuInS_2$ (♣) and In_2S_3 (♦)

Figure 2 shows the *I-t* curves obtained at various cathodic deposition potentials. Cathodic current increased exponentially along with the increase of potential which is due to kinetic limitation of the current. Current-time dependence due to mass transport in term of diffusion causes the concentration gradient in the vicinity of the electrode surface. This involves a gradual expansion of the diffusion layer associated with the depletion of the reactant and hence decreases the slope of the current profile [10].

Analysis of crystal structure

The XRD peaks are found to depend on the deposition potential as shown in Figure 3. It is observed that the intensity of (202) $CuInS_2$ peak decreases with more negative potentials and reaches a minimum value for deposition potential of -0.50 V. The reduction of peak intensity at more negative potential against Ag/AgCl may be due to the hydrogen evolution which suppresses the growth of (202) oriented tetragonal phase. All the $CuInS_2$ peaks are well matched with Joint Committee on Powder Diffraction Standard (JCPDS#75-0106) with d-spacing value of 2.4684 Å. The impurity peak of In_2S_3 exist in all of the samples because copper is difficult to dissociate with other ions at more negative potentials. As the potential is reached at -0.60 V and -0.70 V, the In_2S_3 peak became dominant in the films.

Photoelectrochemical experiment

The current-voltage characteristics of an illuminated semiconductor electrode in contact with redox electrolyte can be obtained easily by adding together the majority and minority current components [11]. Thin films are expected to behave as a semiconductor if they are sensitive to the light, with energy higher than its E_g [12]. Transition of electrons will leave holes in the valence band with a lifetime adequate for them to undergo the electron exchange chemical reaction at the electrode surface or electrolyte interface.

Figure 4 shows the photosensitivity of the samples prepared at –0.30 V potentials. Higher current should be expected in a potential regime corresponding to minority carrier current when the electrode is illuminated and will drop to the value of dark current when light path is blocked. Hence, spikes are formed [14]. By illumination of the film, carriers are excited and the excited minority carriers diffuse to the surface to participate in the electrochemical reaction at the film or electrolyte interface [13]. The spikes are formed at anodic part and this indicates that electrons are minority carriers of the film. Thus, the $CuInS_2$ films prepared were p-type semiconductor with holes as the majority carriers and can be deployed as photocathode in PECs application to undergo a reduction on the electroactive species in the solution.

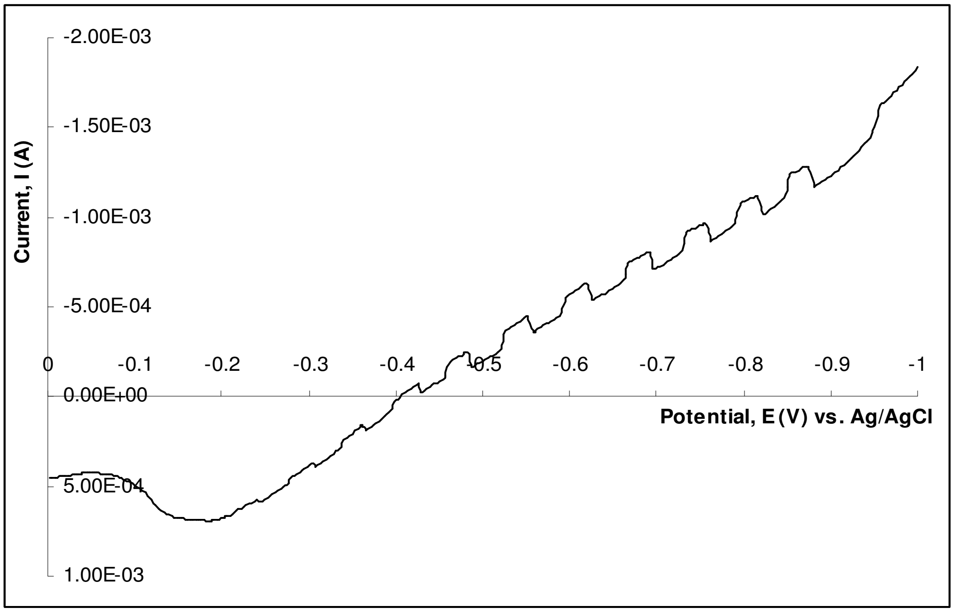

Fig. 4: Photosensitivity of the films prepared at -0.30 V.

Figure 5 is plotted to make the comparison of the photocurrent (I_p) and dark current (I_d) clearer. Overall, the photocurrent is increasing as the potential increased. But, for the sample deposited at -0.50 V, the I_p-I_d is up to 0.12 mA. This shows that the film is quite sensitive to light and suitable to be used as semiconducting material in some devices. Other samples show low I_p-I_d and did not show appreciable increase with the potential.

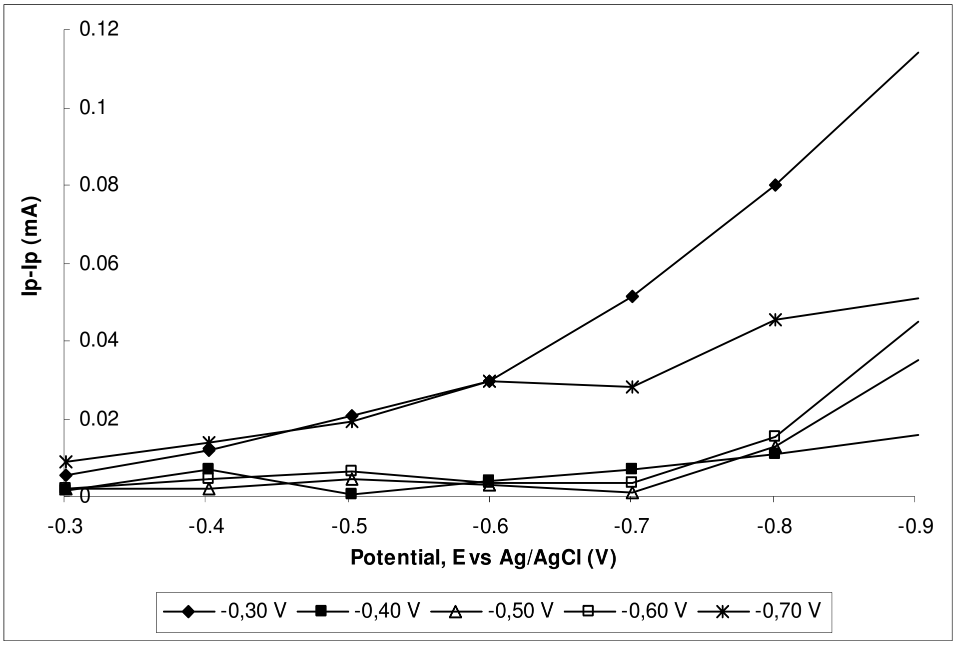

Fig. 5: Comparison of the photocurrent to the dark current [Ip-Id] at selected potentials of the films prepared at different potentials.

Optical properties

The optical band gap of the semiconductor is an important parameter in defining its light absorption behavior. In this quantized process, an electron-hole pair is generated in the semiconductor when a photon of energy hv is absorbed. Optical excitation thus results in a delocalized electron in the conduction band, leaving behind a delocalized hole in the valence band; this is the band-to-band transition [11].

Figure 6 shows the absorbance spectra obtained for the $CuInS_2$ in the region of 300-800 nm. This indicated that the film is active in the visible region of the spectrum. Thus, there is good possibility to deploy it as a visible light energy conversion material. The variation of optical absorption coefficient with wavelength was further analyzed to find out the nature of the electronic transition across the optical band gap. Band gap energy and transition type can be derived by mathematical treatment of the optical absorbance data with Stern equation [15].

$$A = \frac{k(hv - E_g)^{\frac{n}{2}}}{hv}$$

After rearrangement, the above equation gives

$$(Ahv)^{\frac{2}{n}} = k'(hv - E_g)$$

where A is absorbance, ν is a light constant in every unit of wavelength, h is Planck's constant, E_g band gap energy and k', k, n= constant. The band gap energy (E_g) can be obtained by extrapolating the straight line in the plot of $(Ah\nu)^{2/n}$ as the function of hν to the base line where $(Ah\nu)^{2/n}= 0$. As the result, the E_g equals to hν. The n value is 1 for direct-gap transition and 4 for indirect-gap transition. If a straight line graph is obtained for n= 1, it indicates a direct electron transition between states of the semiconductor, whereas the transition is indirect if a straight line graph is obtained for n= 4.

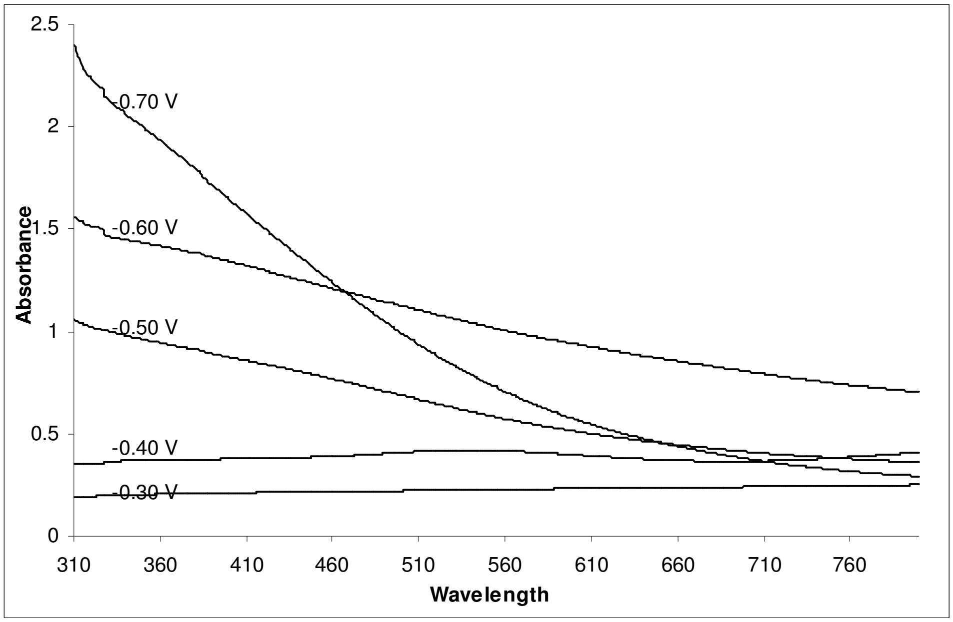

Figure 6: Optical absorbance versus wavelength

From the plotted graph, a linear trend line is apparent when n equals 2 and this indicates direct transition. The band gap energy values were plotted versus deposition potentials as shown in Figure 7. As the deposition potential becomes more cathodic, the band gap energy increase from 1.25 eV to 2.30 eV. Only samples deposited at -0.30 V, -0.40 V and -0.60 V still in agreement with the values reported previously (around 1.50 eV) [16]. For the films deposited at -0.60 V and -0.70 V, their band gap energy value is 2.25 eV and 2.30 eV respectively which are due to the present of In_2S_3 compound in the films. Previous had reported that the band energy of In_2S_3 is 2.3 eV [17]. Beside, the shift of band gap energy relative may be due to the influence of several factors such as grain size, structural parameters and lattice strain, carrier concentration, presence of impurities (or other defects), or even deviation from stoichiometry [17].

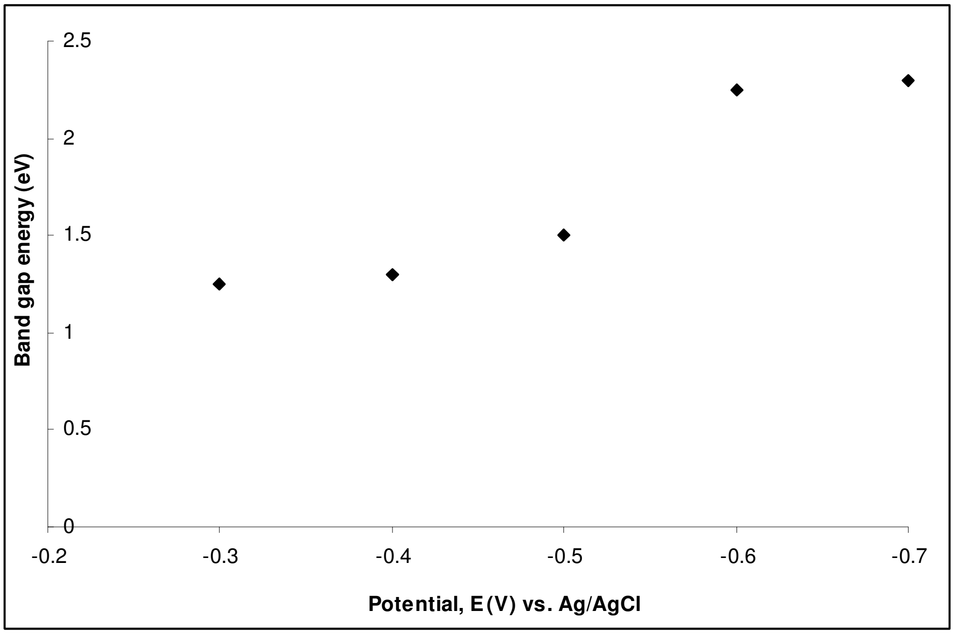

Figure 7: Band gap energy tuning with the cathodic deposition potentials.

Conclusion

$CuInS_2$ thin films have been successfully deposited on ITO by potentiostatic technique. The grown $CuInS_2$ films are polycrystalline in nature. More cathodic potential is not suitable for $CuInS_2$ deposition due to formation of In_2S_3. The optimum deposition potential for the potentiostatically deposition of $CuInS_2$ films is found at -0.50 V. The optical study showed the band gap energy increase from 1.25 to 2.30 eV as the deposition potential increase from -0.30 to -0.70 V which is due to the formation of In_2S_3 phase. The film is observed behavior as p-type semiconductor with direct transition.

Acknowledgement

We thank the Malaysian Government for financial support and University Putra Malaysia for providing research facilities. One of the co-authors (T.S.L.) would like to thank the Ministry of Science, Technology and Innovation for the National Science Fellowship scholarship.

References

1. Henderson, D. O., Mu, R., Ueda, A., Wu, M. H., Gordon, E. M., Tung, Y. S., Huang, M., Keay, J., Feldman, L. C., Hollingsworth, J. A., Buhro, W. E., Harris, J. D., Hepp, A. F. and Raffaelle, R. P. (2001). Optical and structural characterization of copper indium disulfide thin films. *Materials and Design* 22:585-589.
2. Qiu, J., Jin, Z., Wu, W. and Xiao, L. X. (2006). Characterization of $CuInS_2$ thin films prepared by ion layer gas reaction method. *Thin Solid Films* 510:1-5.
3. Hou, X. and Choy, K. L. (2005). Synthesis and characteristics of $CuInS_2$ films for photovoltaic application. *Thin Solid Films* 480-481:13-18.
4. Guha, P., Das, D., Maity, A. B., Ganguli, D. and Chaudhuri, S. (2003). Synthesis of $CuInS_2$ by chemical route: optical characterization. *Solar Energy Materials & Solar Cells* 80:115-130.
5. Asenjo, B., Chaparro, A. M., Gutierrez, M. T. and Herrero, J. (2006). Electrochemical growth and properties of $CuInS_2$ thin films for solar energy conversion. *Thin solid Films* 511:117-120.
6. Sharma, R. K., Rasogi, A. C. and Singh, G. (2004). Electrochemical growth and characterization of manganese telluride thin films. *Materials Chemistry and Physics* 84:46-51.
7. Ghazali, A., Zainal, Z., Hussein, M. Z. and Kassim, A. (1998). Cathodic electrodeposition of SnS in the presence of EDTA in aqueous media. *Solar Energy Materials and Solar Cells* 55:237-249.

8. Grozdanov, I. and Najdoski, M. (1995). Optical and electrical properties of copper sulfide films of variable composition. *Journal of Solid State Chemistry* 114:469-475.
9. Golia, S., Arora, M., Sharma, R. K. and Rastogi, A. C. (2003). Electrochemically deposited bismuth telluride thin films. *Current Applied Physics* 3:195-197.
10. Wang, J. (1993). Controlled-potential techniques. In *Analytical Electrochemistry*, pp27- 29. United States of America: VCH Publisher.
11. Rajeshwar, K. (2001). Fundamentals of semiconductor electrochemistry and phototelectrochemistry. *The University of Texas*.
12. Zainal, Z., Ali, J. A., Kassim, A. and Hussein, M. Z. (2003). Electrodeposition of tin selenide thin film semiconductor: effect of the electrolytes concentration on the film properties. *Solar Energy Materials and Solar Cells* 79:125-132.
13. Fathy, N. and Ichimura, M. (2005). Photoelectrical properties of ZnS thin films deposited from aqueous solution using pulsed electrochemical deposition. *Materials Science and Engineering* 87:747-756.
14. Zainal, Z., Hussein, M.Z., Anuar, K. and Ghazali, A. (1997). Electrodeposition SnS Thin Films from Aqueous Solution. *Journal Material Science Letter* 16:1446-1449.
15. Stern, F. (1963). Elementary theory of the optical properties of solids. *Solid State Physics* 15:299.
16. Martinez, A.M., Fernandez, A.M., Arriag, L.G. and Cano, U. (2006). Preparation and characterization of Cu–In–S thin films by electrodeposition. *Materials Chemistry and Physics* 95:270–274.
17. Mane, R. S. and Lokhande, C. D. (2002). Studies on structural, optical and electrical properties of indium sulfide thin films. *Material Chemistry and Physics* 78:15-17.
18. Marotti, R. E., Guerra, D. N., Bello, C., Machado, G., and Dalchiele, E. A. (2004). Bandgap energy tuning of electrochemically grown ZnO thin films by thickness and electrodeposition potential. *Solar Energy Materials and Solar Cells* 82:85-103.